Journal of Applied Polymer Science

Structural, rheological, and mechanical properties of PA6/SAN/SEBS ternary blend/organoclay nanocomposites

Amir Babaei,[1,2] Ahmad Arefazar[2,3]

[1]Department of Polymer Engineering, Faculty of Engineering, Golestan University, Gorgan, I. R. Iran
[2]Amir Kabir University of Technology, Mahshahr Campus, Mahshahr, I. R. Iran
[3]Department of Polymer Engineering Department, Amir Kabir University of Technology, Tehran, Iran
Correspondence to: A. Arefazar (E-mail: arefazar@aut.ac.ir)

ABSTRACT: The aim of this study was to investigate the effect of nanoclay addition on the morphological and mechanical properties of PA6/SAN/SEBS ternary blend. Two different nanoclays with different modifiers and two different mixing sequences were used to investigate the role of thermodynamic and kinetic, respectively, in the nanoclays localization. XRD, SEM, TEM, melt rheology, tensile and Izod impact tests were used to characterize the nanocomposites. Results of characterization of nanocomposites showed that clay localization is a very influential parameter to determine the type of morphology and, consequently, mechanical properties of ternary/clay nanocomposites. It was demonstrated that presence of nanoclay in the matrix results in the increase of stiffness, while localization of nanoclay at the interface improves the toughness and tensile strength. © 2015 Wiley Periodicals, Inc. J. Appl. Polym. Sci. **2015**, *132*, 41969.

KEYWORDS: blends; clay; morphology; mechanical properties; polyamides

Received 23 September 2014; accepted 6 January 2015
DOI: 10.1002/app.41969

INTRODUCTION

Beginning of 1990 could be considered as the start point of the great attention to the polymer nanocomposites.[1,2] For a decade, there was increasing activities toward the using of polymers as the matrices for nanoparticles either in fundamental research or in industrial exploitation.[3–8] These studies showed that addition of nanofiller generally improved the mechanical properties, heat distortion temperature, and barrier properties, and reduced flammability.[9–11]

Afterward, researchers started to investigate the influence of nanoparticles addition to the polymers blends.[12–21] This topic has attracted a significant attention of researchers. Concerning the polymer blend nanocomposites, the main subjects are principally related to two important roles that these additives can play in the polymer blends. The first is improvement of the various properties such as mechanical, barrier, thermal, flame retardancy, and electrical properties.[12–14] The second objective of the nanoparticles addition to the immiscible polymer blends is how the morphology of the blends is affected by nanoparticles and whether these additives can play the role of compatibilizer in the blends.[15–18] Generally, studies of the researchers indicate that mechanism of action of nanoparticles to modify the morphology, interfacial properties, and performance of immiscible polymer blends relies on their localization, migration, their interactions with polymer components, and the way that these additives disperse within the polymer blend.[19–22]

Contrary to the binary blends, addition of nanofiller such as montmorillonite to a ternary polymeric blend with three distinct phases is a truly new research field. To date, just a few papers have been published on this topic. Kelnar *et al.* studied the effect of two different types of nanoclays on the morphological and mechanical properties of PA6/EPR/PS blend.[23] They reported that addition of clay led to a significant reduction in the size of dispersed particles of minor phases analogously to the corresponding binary blends.[22] Nonetheless, this change resulted in the decrease of toughness of ternary blend. They reported that pre-blending of minor phases with nanoclay could fairly ameliorate the mechanical properties. In another work, Panda *et al.* investigated the influence of MWCNTs addition on the phase morphology and electrical conductivity of PP/PA6/ABS ternary blends.[24,25] They showed that incorporation of MWCNTs into ternary blends, generally, did not alter the type of phase morphology corresponding to respective blends. However, they observed that MWCNTs could act as a compatibilizer, which was manifested in a reduction of average droplet size of the dispersed phases.

Incorporation of nanofiller into a ternary blends can lead to attractive and interesting changes in the morphological and mechanical properties. This arises from the more potential places for the localization of the nanofiller in a ternary blends. The main purpose of this article is to study the effect of clay

Table I. Characteristics of the Prepared Ternary Nanocomposites

Sample code	Used nanoclay	Mixing sequence
NA1	Cloisite 15A	M1
NA2	Cloisite 15A	M2
NB1	Cloisite 30B	M1
NB2	Cloisite 30B	M2

addition on the morphological and, consequently, mechanical properties of PA6/SAN/SEBS ternary blend. In this contribution, we intended to investigate the role of thermodynamic and kinetic in the nanoclay localization by selecting two different types of nanoclays and mixing sequences, respectively.

EXPERIMENTAL

Materials

DSM Chemical Co., (Netherlands) provided polyamide 6 under trade name of Akulon F223 (Density: 1.13 g/cm^3) was used as a matrix. Poly (styrene-co-acrylonitrile) (SAN, 25 wt % AN), SAN-2 (MFI=22 at 220°C, 10 kg) was kindly provided by Ghaed Bassir Petrochemical Co., Iran. Styrene-b-(ethylene-co-butylene)-b-styrene (SEBS) triblock copolymer, Kraton G1652 (29% styrene; molecular weight: styrene block 7000, EB block 37500), was supplied by Shell Chemicals Co., Netherlands. Two kinds of organically modified clays with dimethyl dehydrogenated tallow alkyl ammonium (OMMT, Cloisite15A and Cloisite 30B, Southern Clay Products, USA) were used as layered silicate.

Sample Preparation

All polymers and organoclays were dried for 12 h at 80°C before blending so as to minimize the effects of moisture. All samples were prepared by an internal mixer (Brabender GmbH & Co., Germany) of 60 mL, at a temperature of 230°C; with a rotor speed of 80 rpm for overall mixing time of 10 min. To obtain the standard specimens for the tests of mechanical properties, samples were machined from sheets compression molded at 230°C for 5 min and cooled down under the pressure.

To prepare ternary blends, two different mixing orders were chosen, named M1 and M2 as follows: In M1 sequence, organoclay and PA6 matrix were first blended for 4 min and then other components were added and the mixing was kept on for overall mixing time of 10 min. In M2 sequence, organoclay was first compounded with SAN for 4 min and then other polymers were added. Nanocomposites including Cloisite 15A and Cloisite 30B were named with "NA" and "NB", respectively. Table I summarizes the condition of nanocomposites studied in this work. For comparison, a ternary blend without the organoclay (named "TB") was also prepared. Composition of all samples was PA6/SAN/SEBS/OMMT (70/15/15/5).

Characterization

The structure of the layered silicates in the nanocomposites was analyzed by XRD with a Philips X'pert (Netherlands) PRO with CuKα radiation of wavelength 1.54 Å at room temperature. Measurements were performed in 2θ ranges from 2° to 10° 2θ. For the analysis of morphology, scanning electron microscopy (SEM) was performed using a SERON, AIS-2100 (South Korea) instrument. Cross-sections of cryogenically fractured samples were gold coated in vacuum conditions. The extents of intercalation, exfoliation, and also localization of the clay were monitored by transmission electron microscopy (TEM), JEOL (JEM-2100) at an accelerating voltage of 200 kV using microtomed ultra-thin sections. Microtoming was performed under cryogenic conditions using a microtome equipped with a diamond knife to give super thin sections.

All rheological measurements were performed on a Rheometric Scientific Par Physica MCR 300, a strain-controlled rheometer with cone and plate geometry. All measurements were carried out under the nitrogen atmosphere at 230°C. In all cases, dynamic strain sweeps were initially performed to define the limits of the linear viscoelastic regime. All samples were vacuum dried under 80°C in an oven before the measurements, in order to prevent the moisture-induced degradation. Tensile test was carried out using a Zwick/Roell Z050 (Germany) tensile tester at 50 mm/min according to ASTM D638. Izod impact strength test was done for the notched specimens using an impact tester machine (CEAST Resil Impactor Junior, USA) according to ASTM D256 standard.

RESULTS AND DISCUSSION

X-ray Diffraction

X-ray diffraction is an expedient experimental technique in determining the structure and dispersion of nano silicates in polymer nanocomposites. A shift to lower angles of detected diffraction peak suggests an increase in interlayer spacing or gallery of the nanoclay, which is referred to as intercalation.[2] Disappearance of the nanoclay interlayer diffraction peak indicates possible exfoliation of the nanoclay platelets, and broadening of the peak is considered to be the result of partial exfoliation. The peaks at each diffraction angle are related to the basal spacing of nano platelets via the Bragg's equation ($\lambda=2d\sin\theta$). Figure 1 shows the XRD patterns for the organoclays and prepared nanocomposites. The absence of any distinguishable peak in the XRD patterns of NB nanocomposites [Figure 1(a)] indicates that the exfoliated structure is achieved. Similar result can be observed in the case of NA1 nanocomposite. However, Figure 1(b) reveals that, for NA2 nanocomposite, two weak peaks at $2\theta=4.9$ and 2.6 are observed. This pattern suggests that an intercalated/partial exfoliated microstructure is formed. Combination of XRD measurements and other techniques can help us to achieve a better analysis for the microstructures of nanocomposites.

TEM Analysis

TEM is an effective technique to qualitatively and quantitatively characterize the organoclay dispersion and localization in polymeric blend. Figures 2 and 3 show representative TEM micrographs for nanocomposites prepared using different organoclays and different mixing protocols. Clay layers are marked by arrows in TEM micrographs. Figure 2(a) clearly shows that clay layers are mostly exfoliated in the case of NA1 nanocomposite. This is more obvious when a TEM micrograph at a higher magnification was taken [Figure 2(b)]. Probing the localization of clay layers indicates that some of silicate platelets are localized

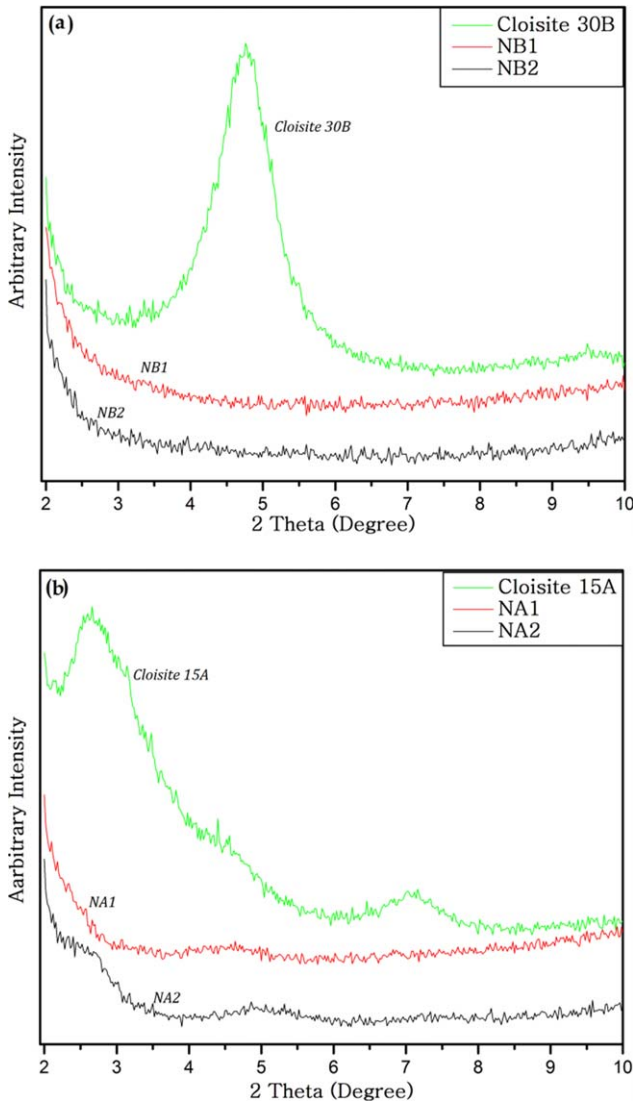

Figure 1. XRD pattern of (a) Cloisite 30B and NB ternary nanocomposites, (b) Cloisite 15A and NA ternary nanocomposites. [Color figure can be viewed in the online issue, which is available at wileyonlinelibrary.com.]

in the PA6 matrix and some of them are placed at the interface of matrix and minor phases. It can be stated that, at first stage of blending, when clay and PA6 are mixed, polyamide exfoliates the clay platelets. In the next stage, when other polymers are added, a part of clay platelets migrate to the interphase of matrix and dispersed phases. This can be ascribed to the lower polarity and affinity of Cloisite 15A to the polar PA6 matrix. In the case of NA2, clay and SAN were first blended and then other polymers were added. TEM micrograph of this nanocomposite shows that intercalated clay layers are mostly localized at the interface of SAN and matrix [Figure 2(c)]. The weak observed peaks in the XRD pattern of this sample, previously shown, can be attributed to these intercalated tactoids. Figure 3 illustrates TEM micrograph of NB2 nanocomposite. It demonstrates that, while SAN and OMMT were firstly blended and then other polymers were added, clay platelets are chiefly dispersed in the matrix. TEM micrograph of NB2 nanocomposite indicate that higher affinity of Cloisite 30B to the matrix, resulting from high polarity of PA6, leads to a great migration of clay layers to the matrix.

Rheological Properties

It is well known that the rheological properties of nanocomposites are sensitive to the surface characteristics and dispersion state of the dispersed phase. Accordingly, it can be considered as a powerful technique to characterize the localization and dispersion state of clay.[26,27] The complex viscosity (η^*) and storage modulus (G') curves of nanocomposites and the ternary blend without clay (TB) as a function of frequency are shown in Figure 4. A general look at these curves indicate that all

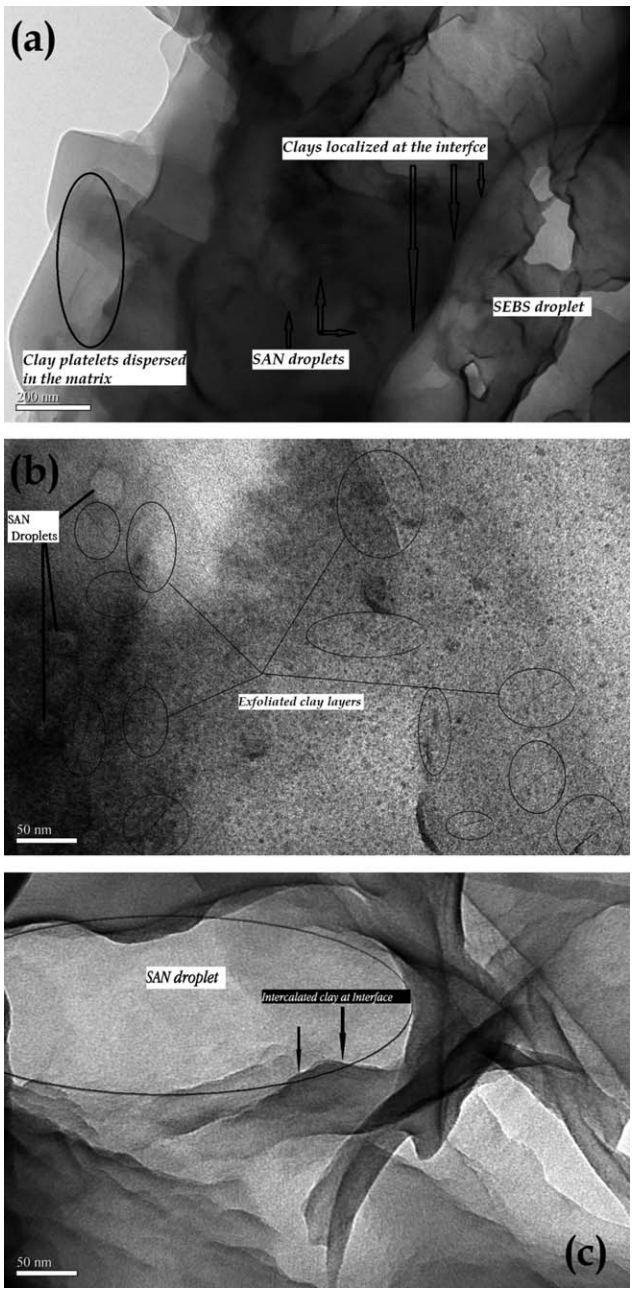

Figure 2. TEM micrographs of ternary nanocomposites; (a) NA1, (b) NA1 at higher magnification, and (c) NA2.

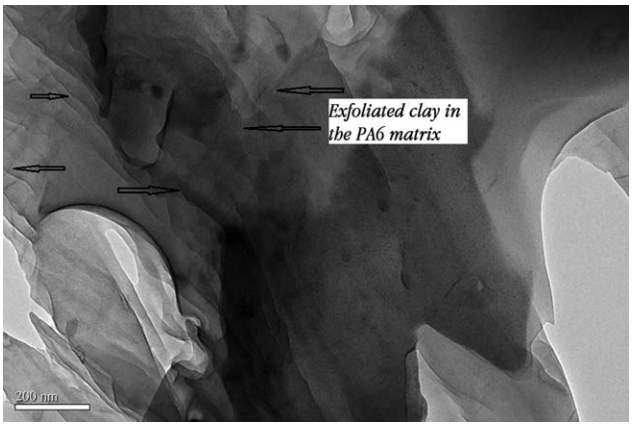

Figure 3. TEM micrographs of NB2 nanocomposite, showing the exfoliated clay layers that are dispersed in the PA6 matrix.

nanocomposites represent an increase in η^* and G' particularly at low frequency regions. It has been frequently reported that polymer/clay interactions, which limit the molecular motions of the polymers, and also the formation of physical clay network structure are responsible for this observations.[27–29] It should also be noted that higher increase of η^* and G' reflect the formation of a stronger or bigger physical network, resulting from the better dispersion of nanoclay platelets in the matrix.

This characteristic allows us to compare the quality of clay dispersion and its localization in a blend. As was stated, XRD and TEM results indicated that clay layers are exfoliated for all the nanocomposites except for the NA2 nanocomposite, which showed an intercalated/partial exfoliated microstructure. However, a fairly significant difference between the rheological measurements of nanocomposites can be observed. It seems that, this difference arises from the different localization of clay layers in the nanocomposites. NB1 and NB2 nanocomposites, in comparison with the neat ternary blend (TB), show highest increase in η^* and G' at low frequency regions. This reflects the formation of strongest physical network of silicate layers in the matrix, among the studied samples. Slightly lower η^* and G' for the NB2 nanocomposite can be correlated to the clay layers located at the interface of PA6 and SAN, during the migration. It can be concluded that, for the NB1 nanocomposite, analogy of thermodynamic (affinity of polar Cloisite 30B to the polar matrix) and kinetic factors (blending of PA6 and nanoclay from the first) lead that most of clay layers are well-exfoliated and dispersed in the matrix. On the other hand, lower increase of η^* and G' for NA nanocomposites at low frequency regions, especially for the nanocomposite NA2, indicate that lower portion of silicate platelets are present in the matrix. Preferential localization of less polar Cloisite 15A clay toward the interface of PA6/SAN, and the kinetic factor (initially blending of clay and SAN) can be considered as the possible reasons for lower η^* and G' in the case of NA2. Rheological measurements indicate that in addition to the dispersion state, location of the clay is also an important factor in governing the rheological properties of polymer blend/clay nanocomposites.

SEM Analysis

To investigate the influence of clay localization on the morphological feature of nanocomposites, scanning electron microscopy was used. SEM images of the etched cryogenic fracture surfaces of the nanocomposites and neat ternary blend without clay are illustrated in Figure 5(a–f), in which SAN was selectively dissolved with dimethyl formamide. SEM micrograph of neat ternary blend demonstrates the formation of core/shell morphology with shell of SAN encapsulating the SEBS phase. It is interesting to notice that addition of two different OMMTs with different types of modifiers results in the formation of two different morphologies. It is observed that while core/shell phase structure is kept fixed for the NB nanocomposites, NA nanocomposites exhibit morphology of two dispersed phases. NA1 nanocomposite exhibits small particles of SAN ($d_n = 0.1$ μm) and larger prolate-spheroid-shaped SEBS particles within PA6 matrix. NA2 nanocomposite shows the same type of the morphology, exhibiting smaller individual SAN particles together with relatively small agglomerates of SEBS particles. These alterations in the phase structure almost certainly arise from the effects associated with localization of nanoclay. In the case of NA1 nanocomposite, TEM and rheological characterizations showed that a notable portion of clay layers are located

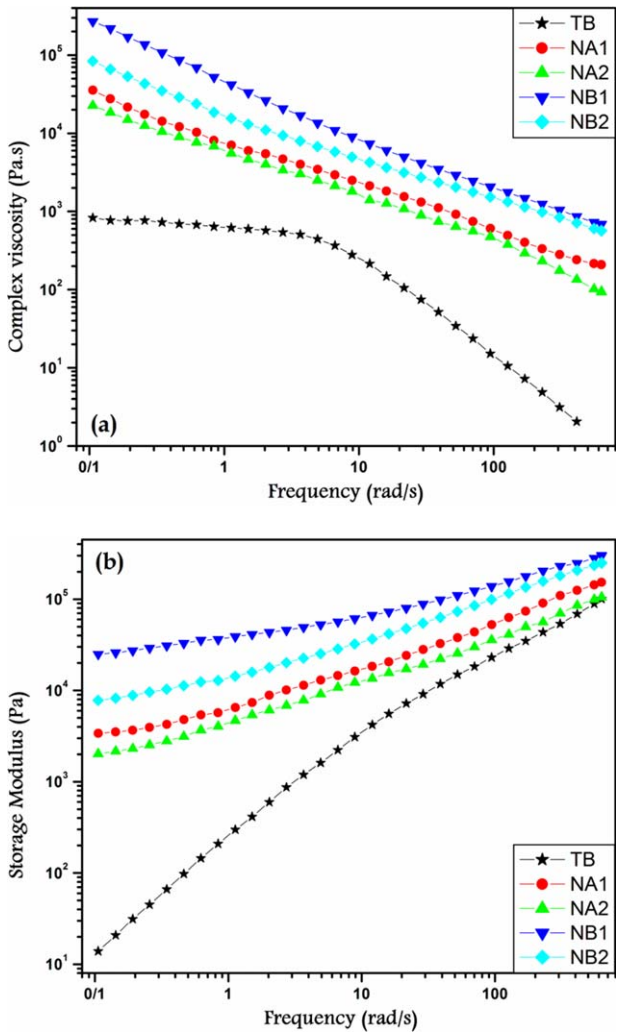

Figure 4. (a) Complex viscosity (η^*) curves of neat ternary blend and prepared nanocomposites. (b) Storage modulus (G') curves of neat ternary blend and prepared nanocomposites. [Color figure can be viewed in the online issue, which is available at wileyonlinelibrary.com.]

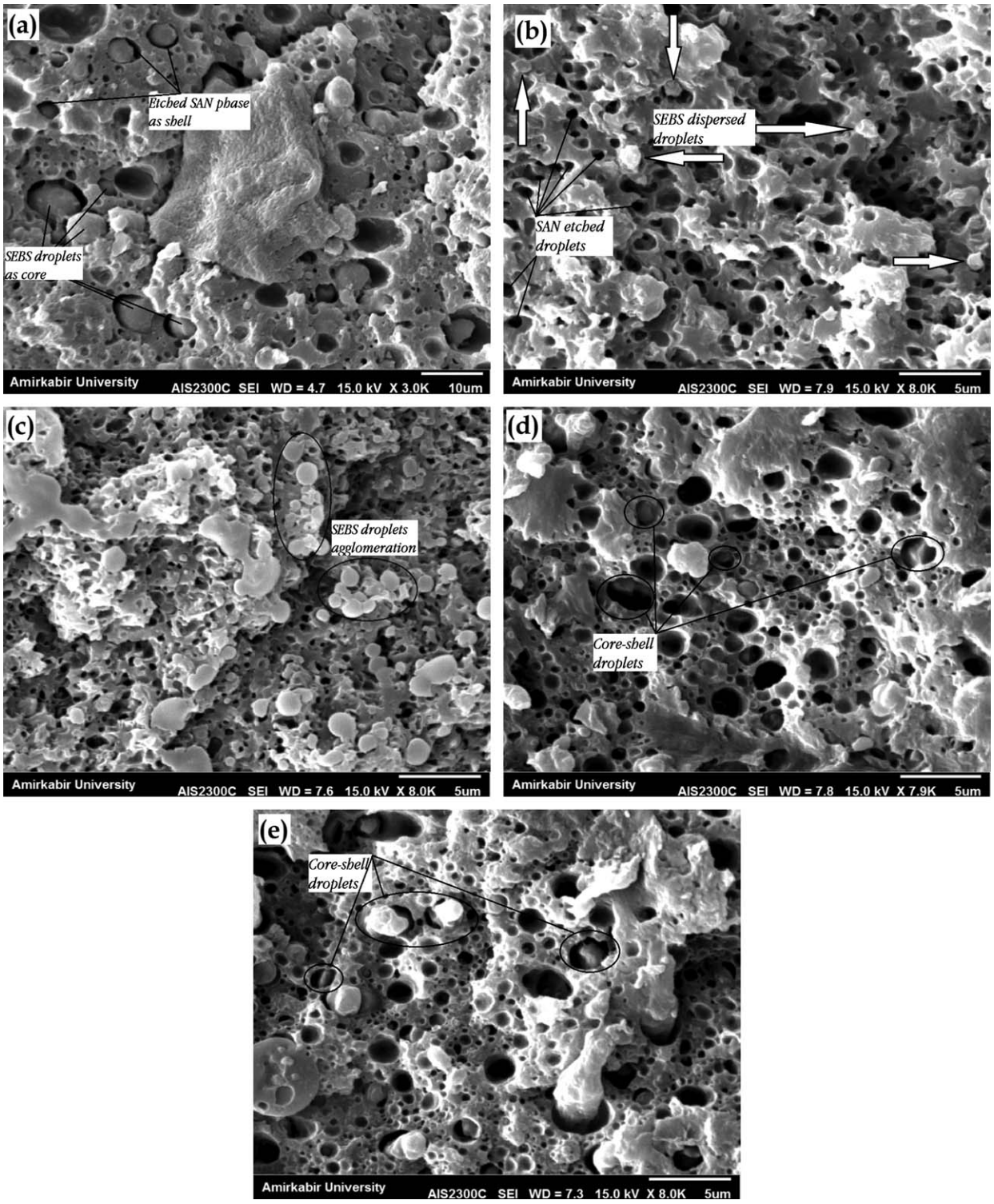

Figure 5. SEM micrographs of SAN phase etched surfaces of: (a) neat ternary blend, (b) NA1, arrows indicate the SEBS particles, (c) NA2, (d) NB1, (e) NB2.

at the interface of matrix and dispersed phases in conjunction with exfoliated layers dispersed in the PA6 matrix. In term of thermodynamic point of view, clay layers localized at the interfaces can act as a compatibilizer to decrease the interfacial tension of matrix and dispersed phases. Compatibilizing effect of nanoclay has been reported by other researchers.[16,29–31] Thus, introduction of nanoclay into the blend as a third component leads to changes in the free energy of blend and, consequently, type of morphology. In addition, clay particles dispersed in the PA6 phase serve as a barrier to delay and minimize the coalescence of dispersed phases.[16–19] This phenomenon refers to the kinetic nature of exfoliated clay platelets. Consequently, for the

Table II. Mechanical Properties of Nanocomposites and Neat Ternary Blend

Sample code	Tensile modulus (MPa)	Tensile strength (MPa)	Impact strength (J/m)
NA1	2735 ± 103	46.15 ± 2.2	56.5 ± 4.8
NA2	2470 ± 56	38.9 ± 1.3	38.3 ± 2.7
NB1	3408 ± 92	32.1 ± 3.1	20.7 ± 0.8
NB2	3245 ± 74	34.8 ± 2.7	25.4 ± 1.8
TB	2570 ± 46	45.1 ± 1.8	28.3 ± 0.7

NA1 nanocomposite, addition of nanoclay may contribute to the compatibility of matrix and minor components (SAN and SEBS) in both thermodynamic and kinetic aspects.[17,21,22] In the case of NA2 nanocomposite, organoclay and SAN were first blended and then, other polymers were added. This mixing sequence favors a greater chance of the clay layers to be placed at the interface of SAN and matrix. Accordingly, less portion of clay platelets are dispersed in the matrix, which was manifested in the lower increase of η^* and G' corresponding to this sample (Figure 4). This preferential localization results in a more pronounced contribution of the thermodynamic compatibilizing effect of clay platelets and limited role for the kinetic aspect.

The phase morphology of PA6/SAN/SEBS ternary blends incorporating Cloisite 30B (NB nanocomposites) are shown in Figure 5(d,e). SEM micrographs of NB nanocomposites clearly reveal that addition of clay does not change the type of morphology in these set of blends. It can be observed that a core/shell morphology is formed, with a lower size of core/shell(s) in comparison with the neat ternary blend. In the previous section, SEM and RMS characterizations suggested that clay platelets of Cloisite 30B have affinity to be dispersed in the PA6 matrix. The existence of a majority fraction of clay layers in the PA6 phase, increasing the viscosity of matrix and obstructing the coalescence of dispersed domains, leads to decrease in the size of core/shell(s).[28–31] It can be inferred that morphological feature of NB nanocomposites is more affected by the kinetic role of clay and its thermodynamic effect is restricted.

Mechanical Properties

Table II shows the mechanical properties of ternary nanocomposites and neat ternary blend. It is well-established that the mechanical properties of blends are highly dependent upon the phase morphology and size of dispersed domains.[32,33] In this work, tensile and impact measurements were carried out to evaluate the possible effects of nanoclays addition on the mechanical properties of the PA6/SAN/SEBS ternary blend. The results demonstrate that the processing protocol and type of used nanoclay have a significant effect on the mechanical properties of nanocomposites. As one can see, although core/shell phase structure is expected to show superior impact strength, the neat PA6/SAN/SEBS ternary blend (TB) exhibits poor toughness properties. This can be ascribed to the poor interfacial interaction between SAN and polar PA6.[34]

Comparing the mechanical results of NB nanocomposites and neat ternary blend indicates that incorporation of nanoclay has no improvement effect on the tensile and impact strength of ternary blend. The clay localization within PA6 as matrix due to lack of contribution toward the compatibilizing of the matrix and dispersed phases could not assist in the modification of interfacial adhesion between the phases and, consequently, the tensile and impact strength of NB nanocomposites. Furthermore, it must also be noted that presence of exfoliated nanoclay platelets in the matrix, restricting the chain deformability and increasing the yield stress, diminishes the impact strength, as generally observed by other researchers.[4,12,14] Slightly better toughness of NB2 nanocomposite can be ascribed to the nanoclay localized at the interface of SAN and PA6 during the migration from SAN to the matrix, manifested in the TEM and RMS tests. In addition, presence of notable fraction of nanoclay in the matrix results in the improvement of modulus of NB nanocomposites. This increase is more considerable for the NB1 nanocomposite, in which thermodynamic and kinetic factors cooperatively cause the highest amount of exfoliated nanoclay layers to be dispersed in the PA6 matrix.

Mechanical results of Table I reveal that NA nanocomposites show higher tensile strength compared with the NB nanocomposites. This can be correlated to the clay localized at the interfaces, which intensifies the interfacial adhesion of matrix and dispersed phases.[21,22,29] Considering SEM, TEM and mechanical results of NA nanocomposites, it is concluded that thermodynamic and kinetic favor the localization of clay platelets at the interfaces rather than the matrix. Localization of clay platelets at the interface causes the change in the interfacial tension of dispersed phases and the matrix, resulting in the change of morphology type, as well as an improvement in the interfacial adhesion of dispersed phases and matrix.

In the case of NA1 nanocomposite, clay platelets kinetically have more chance to be localized at the interface of either PA6/SAN or PA6/SEBS. This results in the improvement of the interfacial adhesion of matrix and dispersed phases, as well as stabilization of the particles of dispersed phases.[29] Accordingly, individual dispersed particles of SAN and SEBS dispersed in the matrix are observed in the SEM micrograph [Figure 5(b)]. However, clay layers are hardly placed at PA6/SEBS interface for the NA2 nanocomposite. Therefore, a relatively little agglomeration of SEBS particles is observed [Figure 5(c)]. Lower tensile and impact strength of NA2 in comparison with the NA1 can be ascribed to the agglomerates of SEBS particles. These agglomerates are capable to form the macrovoids from which matrix cracks can initiate, resulting in the decrease of tensile and impact strength. Lower modulus of NA nanocomposites, as expected, is the consequence of less presence of clay platelets in the PA6 matrix.

It has been repeatedly reported that elongation at break can be considered as a measure to evaluate the adhesion between the phases in a blend. Figure 6 depicts the elongation at breaks of studied samples. It is clearly observed that, in analogy with tensile and impact strength, NA1 nanocomposite exhibits the highest elongation at break, emphasizing the compatibilizing role of clay platelets localized at the

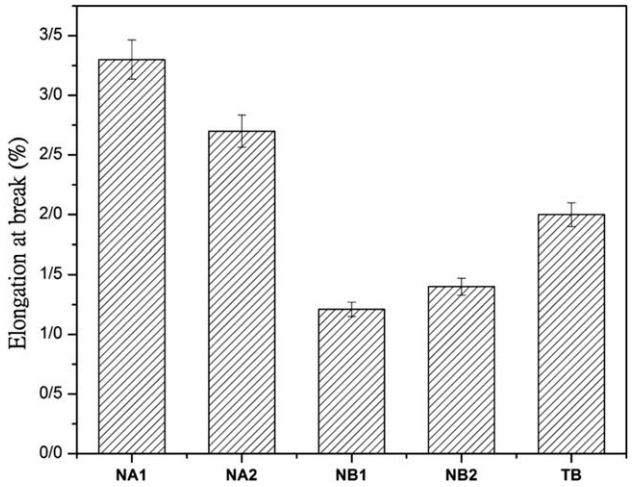

Figure 6. Elongations at breaks of neat ternary blend and prepared ternary nanocomposites.

interfaces. As a conclusion, NA1 nanocomposite, which demonstrates a fair distribution of clay layers in the matrix and also at the interfaces of dispersed phases, exhibits an acceptable stiffness–toughness balance.

CONCLUSION

In this work, the relationship between the localization of clay in PA6/SAN/SEBS ternary nanocomposite and morphological–mechanical properties was studied. To explore the role of thermodynamic and kinetic in the localization of clay, two different clays with different modifiers and two mixing sequences were used. Results showed that addition of clay led to considerable changes in the morphological and also mechanical properties of ternary blend. It was demonstrated that affinity of clay toward a phase (thermodynamic factor) is more influential parameter in comparison with the mixing sequence (kinetic factor) in the localization of clay layers. Rheological analysis suggested the enhancement of complex viscosity and storage moduli of the nanocomposites compared to the neat ternary blend, especially when used nanoclay preferred to be chiefly located in the matrix. SEM and TEM micrographs showed that when a considerable portion of nanoclay platelets prefer to be dispersed in the matrix, core/shell phase structure of neat ternary blend was not changed. On the other hand, localization of nanoclay at the interface resulted in the change of morphology type to two dispersed phases. Mechanical assessments demonstrated superior stiffness for the nanocomposites in which nanoclay layers are mostly dispersed in the matrix. However, increased toughness and strength were observed to be greatest when the organoclay was located in the interface of matrix and dispersed minor phases. It was also illustrated that the best balanced stiffness–toughness properties is achieved when nanoclay layers are located in either the matrix or the interface of both the dispersed phases.

ACKNOWLEDGMENTS

We gratefully thank the Iran National Science Foundation INSF for the generous financial supports

REFERENCES

1. Okada, A.; Kawasumi, M.; Usuki, A.; Kojima, Y.; Kurauchi, T.; Kamigaito, O. *MRS Symp. Proceedings* **1990**, *171*, 45.
2. Giannelis, E. P. *Polym. Adv. Mater.* **1996**, *8*, 29.
3. Al-Mulla, A. *Int. J. Polym. Anal. Charact.* **2009**, *14*, 540.
4. Modesti, M.; Lorenzetti, A.; Bon, D.; Besco, S. *Polymer* **2005**, *46*, 10237.
5. Al-Kandary, Sh.; Ali, A. A. M.; Ahmad, Z. *J. Appl. Polym. Sci.* **2005**, *98*, 2521.
6. Wu, T. M.; Chu, M.-S. *J. Appl. Polym. Sci.* **2005**, *98*, 2058.
7. Khorasani, M. M.; Ghaffarian, S. R.; Goldansaz, S. H.; Mohammadi, N.; Babaie, A. *Comput. Sci. Technol.* **2010**, *70*, 1942.
8. Babaei, A.; Ghaffarian, S. R.; Khorasani, M. M.; Baseghi, S. *J. Macromol. Sci. B: Polym. Phys.* **2012**, *51*, 481.
9. Krishnamacharia, P.; Zhanga, J.; Loua, J.; Yana, J.; Uitenham, L. *Int. J. Polym. Anal. Charact.* **2009**, *14*, 336.
10. Dong, Y.; Bhattacharyya, D.; Hunter, P. *J. Comp. Sci. Technol.* **2008**, *68*, 2864.
11. Sanchez-Olivares, G.; Sanchez-Solis, A.; Camino, G.; Manero, O. *Express Polym. Lett.* **2008**, *2*, 569.
12. Yoo, Y.; Tiwari, R. R.; Yoo, Y. T.; Paul, D. R. *Polymer* **2010**, *51*, 4907.
13. Xiang, F.; Wang, Y.; Shi, Y.; Huang, T.; Chen, C.; Peng, Y.; Wang, Y. *Polym. Int.* **2012**, *61*, 1334.
14. Ville, J.; Mederic, P.; Huitric, J.; Thierry, A. *Polymer* **2012**, *53*, 1733.
15. Fenouillot, F.; Cassagnau, P.; Majeste, J. C. *Polymer* **2009**, *50*, 1.
16. Oliveira, A. D.; Larocca, N. M.; Paul, D. R.; Pessan, L. A. *Polym. Eng. Sci.* **2012**, *52*, 1.
17. Moghbelli, E.; Sue, H. J.; Jain, S. *Polymer* **2010**, *51*, 4231.
18. Martins, C. G.; Larocca, N. M.; Paul, D. R.; Pessan, L. A. *Polymer* **2009**, *50*, 1743.
19. Eslami, H.; Musa, R. K. *J. Appl. Polym. Sci.* **2013**, *127*, 2290.
20. Dasari, A.; Yu, Z. Z.; Mai, Y. W. *Polymer* **2005**, *46*, 5986.
21. Gonzalez, I.; Eguiazabal, J. I.; Nazabal, J. *Eur. Polym. J.* **2008**, *44*, 287.
22. Kelnar, I.; Khunova, V.; Kotek, J.; Kapralkova, L. *Polymer* **2007**, *48*, 5332.
23. Panda, B.; Bhattacharyya, A. R.; Kulkarni, A. *Polym. Eng. Sci.* **2011**, *51*, 1550.
24. Panda, B.; Bhattacharyya, A. R.; Kulkarni, A. *J. Appl. Polym. Sci.* **2013**, *127*, 1433.
25. Kelnar, I.; Rotrekl, J.; Kotek, J.; Kapralkova, L.; Hromadkova, J. *Eur. Polym. J.* **2009**, *45*, 2760.
26. Krishnamoorti, R.; Giannelis, E. P. *Macromolecules* **1997**, *30*, 4097.
27. Ren, J.; Silva, A. S.; Krishnamoorti, R. *Macromolecules* **2000**, *33*, 3739.
28. Bagheri, S.; Fox, D.; Chen, Y.; Geever, L. M.; Khavandi, A.; Bagheri, R.; Higginbotham, C. L.; Zhang, H.; Chen, B. *Comp. Sci. Technol.* **2012**, *72*, 1697.

29. Elias, L.; Fenouillot, F.; Majeste, J. C.; Alcouffe, P.; Cassagnau, P. *Polymer* **2008**, *49*, 4378.
30. Chow, W. S.; Bakar, A. A.; Ishak, Z. A. M.; Karger-Kocsis, J.; Ishiaku, U. S. *Eur. Polym. J.* **2005**, *41*, 687.
31. Calcagno, C. I. W.; Mariani, C. M.; Teixeira, S. R.; Mauler, R. S. *Comp. Sci. Technol.* **2008**, *68*, 2193.
32. Das, V.; Kumar, V.; Singh, A.; Gautam, S. S.; Pandey, A. K. *Polym. Plast. Technol. Eng.* **2012**, *51*, 446.
33. Das, V.; Gautam, S. S.; Pandey, A. K. *Polym. Plast. Technol. Eng.* **2011**, *50*, 825.
34. Nair, S. V.; Subramaniam, A.; Goettler, L. A. *J. Mater. Sci.* **1998**, *33*, 3455.